NACA TN 2528
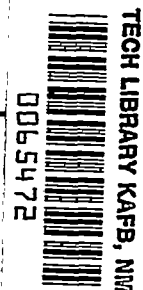
8914

NATIONAL ADVISORY COMMITTEE FOR AERONAUTICS

TECHNICAL NOTE 2528

A METHOD FOR PREDICTING THE UPWASH ANGLES INDUCED

AT THE PROPELLER PLANE OF A COMBINATION OF

BODIES WITH AN UNSWEPT WING

By Paul F. Yaggy

Ames Aeronautical Laboratory
Moffett Field, Calif.

NACA

NATIONAL ADVISORY COMMITTEE FOR AERONAUTICS

TECHNICAL NOTE 2528

A METHOD FOR PREDICTING THE UPWASH ANGLES INDUCED

AT THE PROPELLER PLANE OF A COMBINATION OF

BODIES WITH AN UNSWEPT WING

By Paul F. Yaggy

SUMMARY

A method has been developed for predicting the upwash angles induced at the horizontal center line of the propeller disk of the twin-engine airplane considered in NACA TN 2192, 1950. The method treats each component separately and includes approximations for the interference effects of the other components. Lifting-line theory was used to determine the wing-induced upwash angles. The theory used for the nacelle is an extension of the airship theory of NACA TM 574, 1930. The fuselage-induced upwash angles were determined by means of a solution for the transverse flow about an infinite elliptic cylinder.

The boundary conditions of the airship theory used to predict the upwash angles due to the nacelle of the airplane were not strictly satisfied. Therefore, a comparison was made of predicted and measured upwash angles for an isolated nacelle which approximated in shape that of the airplane of NACA TN 2192. The comparison of the computed values of upwash angle with the measured values showed satisfactory agreement.

Comparison of the computed and measured total upwash angles showed that the method satisfactorily accounted for the upwash angles induced by the airplane. Although the method was developed for a specific airplane, the method should be applicable to similar airplanes; the conditions of similarity are defined in the report.

Modifications to the method are suggested which, it is believed, would make it applicable to certain dissimilar airplanes.

INTRODUCTION

It has been shown in investigations of first-order vibratory stresses in propellers (references 1 and 2) that, for subcritical speeds, the oscillating aerodynamic loadings which excited these stresses could

be predicted by steady-state propeller theory if the flow field were known. It is apparent from the data of reference 1 that, of the flow-field parameters, the upwash angles measured along the horizontal center line of the propeller disk had the largest effect on the oscillating aerodynamic loading. It was shown in reference 1 that the upwash angles measured along this center line were in excess of the computed wing-induced upwash angles, and the variation had a considerably different shape. The differences were such as to indicate that they were due to the nacelle, primarily, and to the fuselage to a lesser degree. The development and application of a method for predicting the upwash angles for the airplane considered in reference 1 was the purpose of the investigation reported herein.

In order to avoid the complications of an exact theoretical method, an approximate method was developed whereby available theory for each component of the combination was used with certain simple approximations to account for interference effects. Since the nacelle did not conform to the restrictions of the theory, it was necessary to obtain data suitable for determining the applicability of the theory to the nacelle tested. The general applicability of the method is discussed.

NOTATION

A_1 nacelle inlet area, at station 0

$\dfrac{m_1}{m_0}$ Nacelle inlet mass-flow ratio $\left(\dfrac{\rho_1\, A_1\, V_1}{\rho_0\, A_1\, V_0} \right)$

r distance along any radial line from the longitudinal axis of a body

R radius of a body at any point x on the longitudinal axis

V_0 free-stream velocity

V_1 average velocity at the nacelle inlet

ΔV_i incremental transverse-flow velocity

V_Ω velocity at a point in a transverse plane normal to a radial line extending from a body axis through the point

W cross velocity ($W = V_0 \sin \alpha$)

x longitudinal distance from any doublet element on the body longitudinal axis to a transverse plane containing the point at which the upwash angle is to be computed, positive aft from the doublet element

α_G geometric angle of attack of the thrust axis with respect to the free stream

α angle of attack of the longitudinal axis of a body with respect to the local air-stream direction

ϵ angle of upwash measured from the free-stream direction in a plane parallel to the model vertical plane of symmetry

θ $\tan^{-1} \frac{r}{x}$

μ moment per unit length of a doublet element

ρ_0 mass density of air in the free stream

ρ_1 mass density of air at the nacelle inlet

Φ potential function

Ω angular position about the body axis, measured counterclockwise from the upper vertical position as seen from the front

   The symbols r, R, V_0, V_Ω, W, x, α, ϵ, θ and Ω are further defined in figure 1.

Subscripts

LE   leading end of a body

TE   trailing end of a body

MODEL AND APPARATUS

   The nacelle tested had approximately the same shape as the nacelle of the airplane (fig. 2) and was formed by adding a suitable afterbody to the engine cowling of the port nacelle of the airplane. Two modifications to this basic nacelle were also made. One was the addition of a conical nose fairing to the basic nacelle; the other, the addition of a conical spinner. Drawings of the basic and modified nacelles are shown in figure 3. Photographs of each of the three nacelles mounted in the Ames 40- by 80-foot wind tunnel are shown in figure 4.

   For all three nacelles, the survey plane was located 8 inches ahead of the basic nacelle leading edge. The instrumentation, the method of surveying, and the location of the survey plane were the same as described in reference 1.

TESTS AND RESULTS

Measurements of the upwash angle along the horizontal center line of the propeller disk were made for each of the three nacelles. The surveys extended 70.5 inches from the nacelle axis. Data were obtained throughout an angle-of-attack range of 0° to 16° at a tunnel speed of approximately 140 miles per hour. The inlet mass-flow ratio for the nacelle with conical spinner was 0.7 and for the basic nacelle was 0.2.

The test data for the nacelles are presented in figure 5. Corrections to the data for tunnel-wall effects were negligible.

METHOD

The following theories and procedures were used in calculating the upwash angles induced at the horizontal center line of the propeller disk by the various components of the airplane. The total upwash angle was then calculated by summation of the results obtained for each component.

Wing-Induced Upwash Angles

Lifting-line theory was used to determine the wing-induced upwash angles. The span load distribution was approximated by a system of horseshoe vortices. The upwash angle was then calculated for each vortex by the equations given by Glauert in reference 3. A summation of these angles gave the total upwash angle induced by the wing.

The span load distribution was taken to be that for the wing alone. This was justified since computation showed the large differences between wing-alone and wing-nacelle-fuselage span loadings to result in negligible changes in upwash. Similar agreement was noted for another wing-fuselage-nacelle combination in which the wing had a greatly different plan form.

Nacelle-Induced Upwash Angles

The theory used for the nacelle was that of reference 4, extended to obtain an expression for the upwash angles induced by a body at an angle of attack. The expression for the upwash angle in the horizontal plane of symmetry is derived in the appendix and is as follows:

$$\epsilon = \frac{\alpha}{2r^2} \int_{\theta_{LE}}^{\theta_{TE}} R^2 \sin \theta d\theta$$

This expression is for closed bodies of revolution. The basic nacelle of the airplane deviated from the boundary condition in that there was flow through the nacelle. Therefore, the applicability of the theory for calculating the upwash angle for this nacelle was determined by a comparison of computed and measured angles of upwash. The theory was further evaluated by comparison of computed and measured values of upwash angle for the nacelle with the conical fairing, or with the conical spinner. The former case conformed to the boundary conditions of the theory. In computing the upwash angles for the nacelles with inlets, the surface was considered to continue across the opening. The measured nacelle upwash angles indicated that the thrust axis, which was chosen as the reference axis, was tilted down 2° with respect to the nacelle longitudinal axis. This was taken into account when computing upwash angles for a given geometric angle of attack. Comparisons of experiment and theory are presented in figure 6 and satisfactory agreement is shown.

Since the nacelle, when in combination with the wing, was in the upwash field of the wing, it was assumed that it was at an effective angle of attack. This effective angle was taken to be the sum of the geometric angle of attack and the wing-induced upwash angle on the center line of the nacelle at the propeller plane. Therefore, the upwash was computed for the nacelle at the effective angle of attack.

Fuselage-Induced Upwash Angles

In determining the fuselage-induced upwash angles the fuselage was considered to be an infinite elliptic cylinder. This approach is reasonable because the fuselage extended well forward of the propeller plane and the area of the cross sections, which were approximately elliptic in shape, varied only slightly in the vicinity of the propeller plane. Further, since the upwash angle contribution of the fuselage was relatively small, any error introduced by this procedure would not be significant.

The upwash angles due to an inclined infinite elliptic cylinder were determined from values of incremental transverse-flow velocity about such a cylinder. The expression used for the upwash angle is:

$$\epsilon = \left(\frac{\Delta V_i}{W}\right) \alpha$$

Values of the ratio $\Delta V_i/W$ can be found in figure 7 of reference 5. It should be noted a difference in notation exists wherein W of the present report corresponds exactly to V_o of reference 5.

The reasoning regarding the effective angle of attack of the fuselage, when in combination with the wing, followed that used for the nacelle. Thus, the fuselage was assumed to be at an effective angle of attack which was taken to be the geometric angle of attack plus the wing-induced upwash angle on the fuselage center line at the propeller plane. The geometric angle of attack was measured with respect to the slope of the mean-thickness line of the fuselage at the plane of the propeller. For an angle of attack of the thrust axis of $0°$, the geometric angle of attack of the fuselage was $-2°$.

DISCUSSION

Evaluation of the Method

The method was applied to determine the upwash angles induced by the complete airplane when $\alpha_G = 10°$. The computed values of upwash angles were corrected to wind-tunnel conditions in order to compare them with the experimental results presented in reference 1. The spanwise variations of the computed and measured total upwash angle are shown in figure 7. To indicate the contribution of each part of the airplane to the total upwash angle, the spanwise variations of upwash angle computed for each of the components are also shown. Comparison of the computed and measured total upwash angles shows that the method accounted for the combined effects of the components.

Application of the Method to Similar Configurations

The foregoing comparison justifies examination of the general applicability of the method presented herein. It would be expected to give satisfactory prediction of the upwash angles for airplanes which are similar to the reference airplane to the extent that:

1. The propeller plane is at least 60-percent chord ahead of the wing leading edge.

2. The wing is unswept and has a moderate or high aspect ratio.

3. The bodies are circular in cross section if the leading edges are behind the propeller plane (nacelles, a fuselage, external stores or a fuselage of a single-engine tractor-type airplane), cr if the

leading edges are less than three maximum mean diameters ahead of the propeller (spinners, fuselage or external stores).

4. Bodies which extend a distance in excess of three maximum mean diameters ahead of the propeller plane have nearly constant cross sections in the vicinity of that plane, and have circular or nearly elliptical cross sections.

5. In the case of multiple bodies, the center lines of any two bodies are separated by at least one and one-half maximum diameters of the body with larger diameters.

Extension of the Method to Dissimilar Configurations

It is believed that airplanes which do not comply with these restrictions can be handled by making the following suggested modifications to the method. If the wing is swept, a wing theory such as that of reference 6 should be used. A body of elliptical cross section, the nose of which is behind or less than three maximum mean diameters ahead of the propeller plane, may require a theoretical treatment different from that used in the present method for a body with circular cross section. If the bodies of an airplane are large and relatively close to each other, it will be necessary, when determining the effective angle of attack of one body, to consider the induced-upwash angles of the other body or bodies. It is not known how close the propeller plane may approach the wing leading edge before account must be taken of the fact that the wing vorticity is distributed chordwise and the fact that the bodies lie in a varying upwash field.

CONCLUDING REMARKS

The method presented herein satisfactorily predicted the upwash angles induced at the horizontal center line of the propeller disk of the airplane described in reference 1. The method would be expected to give satisfactory results for similar airplanes. Modifications to the method were suggested which, it is believed, will make it applicable to airplanes which differ in certain respects from the specific airplane discussed herein.

Ames Aeronautical Laboratory
        National Advisory Committee for Aeronautics
                Moffett Field, Calif., August 24, 1951

APPENDIX

DERIVATION OF THE EXPRESSION FOR THE UPWASH ANGLE INDUCED

IN THE HORIZONTAL MERIDIAN PLANE BY A BODY OF REVOLUTION

In reference 4, it is shown that the transverse flow about an infinitely long cylinder may be obtained by covering the longitudinal axis (axis of revolution) with doublets of moment per unit length, μ. The potential function of a doublet element of strength μdx is

$$d\Phi = \frac{-\mu}{4\pi r} \cos \Omega \sin \theta d\theta \qquad (1)$$

The potential function for the distribution of doublets along the longitudinal axis of a body of finite length may be obtained by integrating between the limits θ_{LE} to θ_{TE} where the limits are the values of θ at the upstream and downstream ends, respectively. Thus, integrating equation (1) between these limits yields the expression

$$\Phi = \frac{-\cos \Omega}{4\pi r} \int_{\theta_{LE}}^{\theta_{TE}} \mu \sin \theta d\theta \qquad (2)$$

and differentiating equation (2) with respect to Ω yields

$$\frac{d\Phi}{d\Omega} = \frac{\sin \Omega}{4\pi r} \int_{\theta_{LE}}^{\theta_{TE}} \mu \sin \theta d\theta \qquad (3)$$

Now the expression for the velocity V_Ω is

$$V_\Omega = \frac{1}{r} \frac{d\Phi}{d\Omega} \qquad (4)$$

Substituting equation (4) in equation (3), we have

$$V_\Omega = \frac{\sin \Omega}{4\pi r^2} \int_{\theta_{LE}}^{\theta_{TE}} \mu \sin \theta d\theta \qquad (5)$$

Let us assign a strength $\mu = 2\pi R^2 W$ to each of the doublets. Now, if R is assumed constant, integration of equation (5) yields the tangential velocity about a cylinder of radius R. If, for a body with varying radius as the bodies under consideration, we consider each section to be one of an infinitely long cylinder and allow μ to vary as

R, the expression for the velocity V_Ω, becomes

$$V_\Omega = \frac{\sin\Omega\, V_0 \sin\alpha}{2r^2} \int_{\theta_{LE}}^{\theta_{TE}} R^2 \sin\theta d\theta \qquad (6)$$

Since for small angles of attack of the longitudinal axis the vertical velocity is nearly equal to the velocity V_Ω, the upwash angle in the horizontal plane $\Omega = 90^\circ$ is

$$\epsilon = \frac{V_\Omega}{V_0} = \frac{\alpha}{2r^2} \int_{\theta_{LE}}^{\theta_{TE}} R^2 \sin\theta d\theta \qquad (7)$$

As has been shown by Munk and von Kármán, for calculations of potential flow in the vicinity of the nose of a body, only the forward half-body need be considered. The body downstream of the midsection is therefore assumed to continue to infinity with the radius of the midsection. Thus, the upper limit θ_{TE} may be assumed to be π.

The integration is accomplished numerically to the midsection, after which it is a simple integral because of the assumed constant radius.

REFERENCES

1. Roberts, John C., and Yaggy, Paul F.: A Survey of the Flow at
      the Plane of the Propeller of a Twin-Engine Airplane.
      NACA TN 2192, 1950.

2. Rogallo, Vernon L., Roberts, John C., and Oldaker, Merritt R.:
      Vibratory Stresses in Propellers Operating in the Flow Field of
      a Wing-Nacelle-Fuselage Combination. NACA TN 2308, 1951.

3. Glauert, H.: The Elements of Aerofoil and Airscrew Theory.
      Cambridge, England, the University Press, Ch. XII, 2d ed., 1947.

4. von Kármán, Theodor: Calculation of Pressure Distribution on
      Airship Hulls, NACA TM 574, 1930.

5. Robinson, Russell G., and Wright, Ray H.: Estimation of Critical
      Speeds of Airfoils and Streamline Bodies. NACA ACR March, 1940.

6. DeYoung, John and Harper, Charles W.: Theoretical Symmetric Span
      Loading at Subsonic Speeds for Wings Having Arbitrary Plan Form.
      NACA Rep. 921, 1948. (Formerly issued as NACA TN's 1476, 1491,
      and 1772)
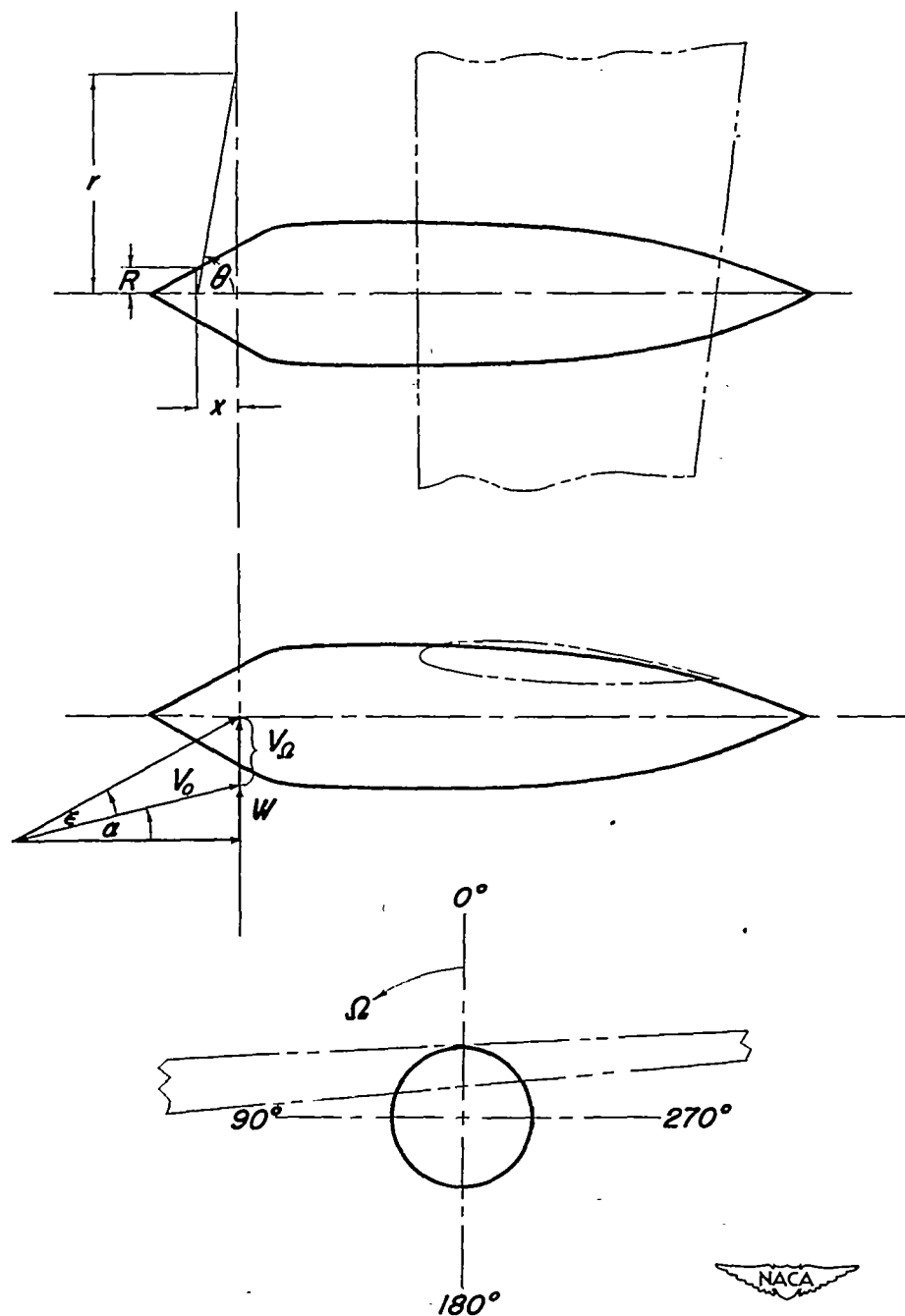
*Figure 1.- Geometric characteristics of the flow pa-
rameters relative to the horizontal center line
of a propeller plane. All angles and vectors are
shown positive.*

Figure 2.- Geometric characteristics of the twin-engine, fighter-type airplane.

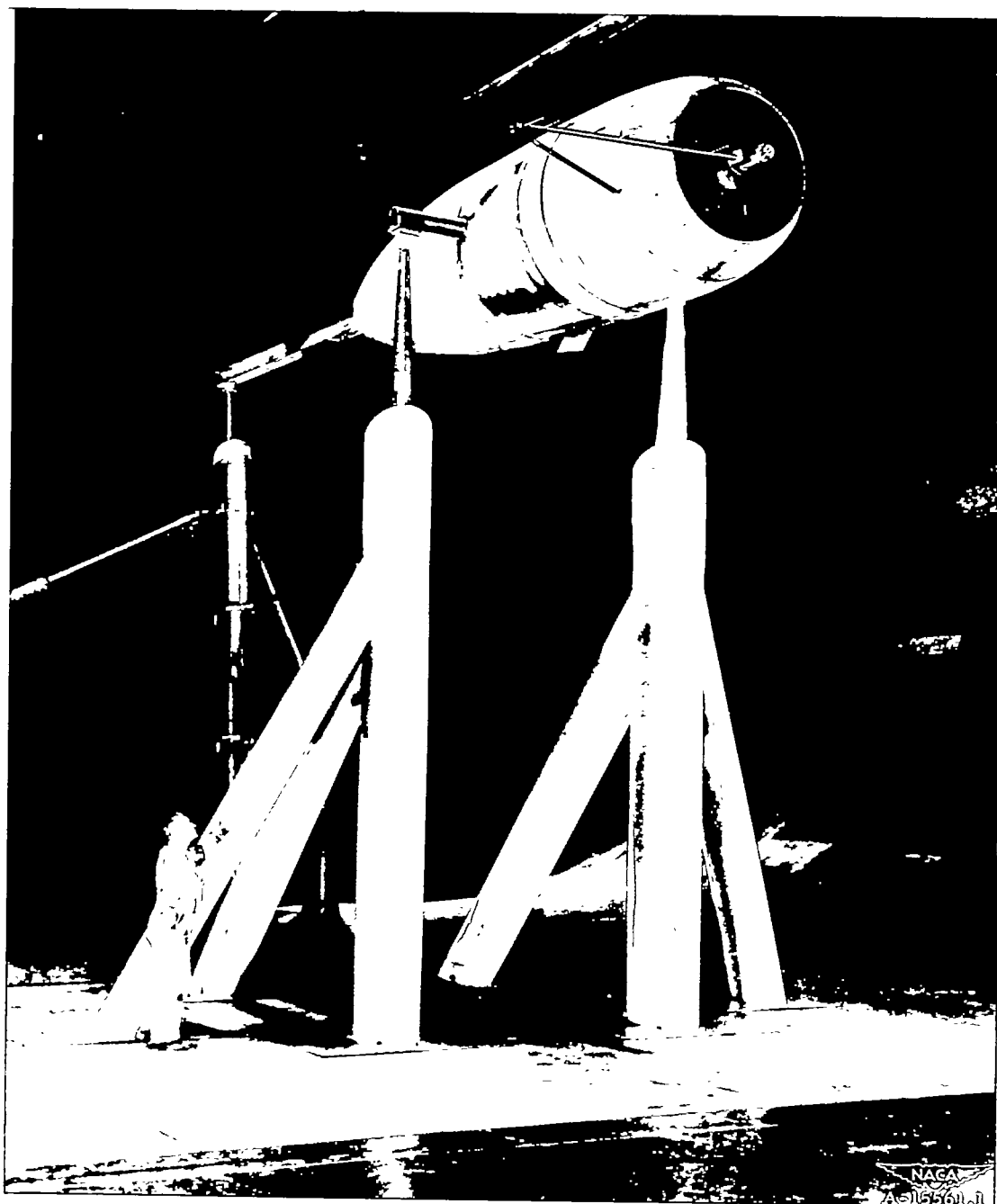Figure 3.- Geometric characteristics of the three nacelles.

All dimensions are in inches.
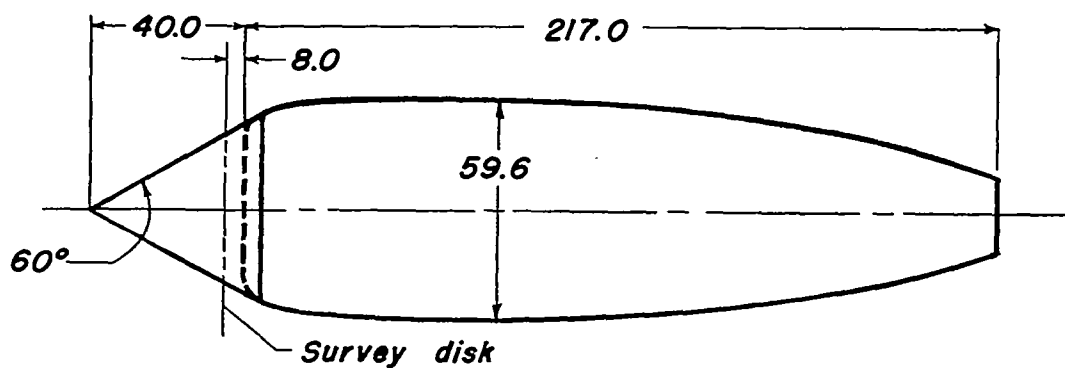
(b) Nacelle with conical fairing.
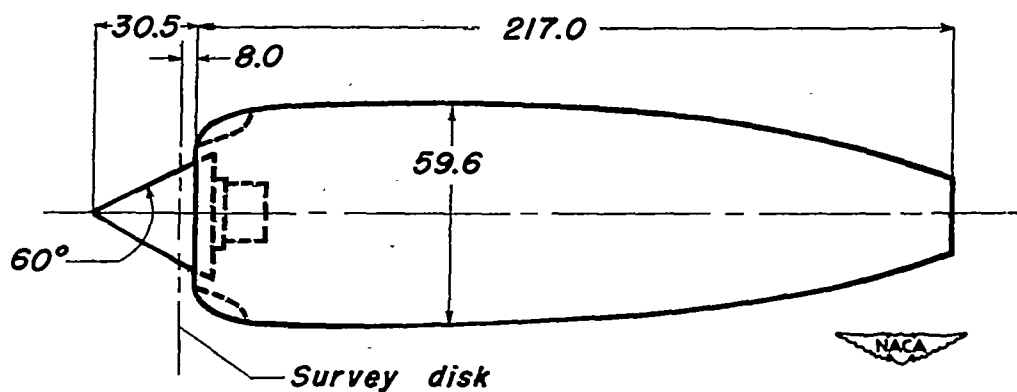
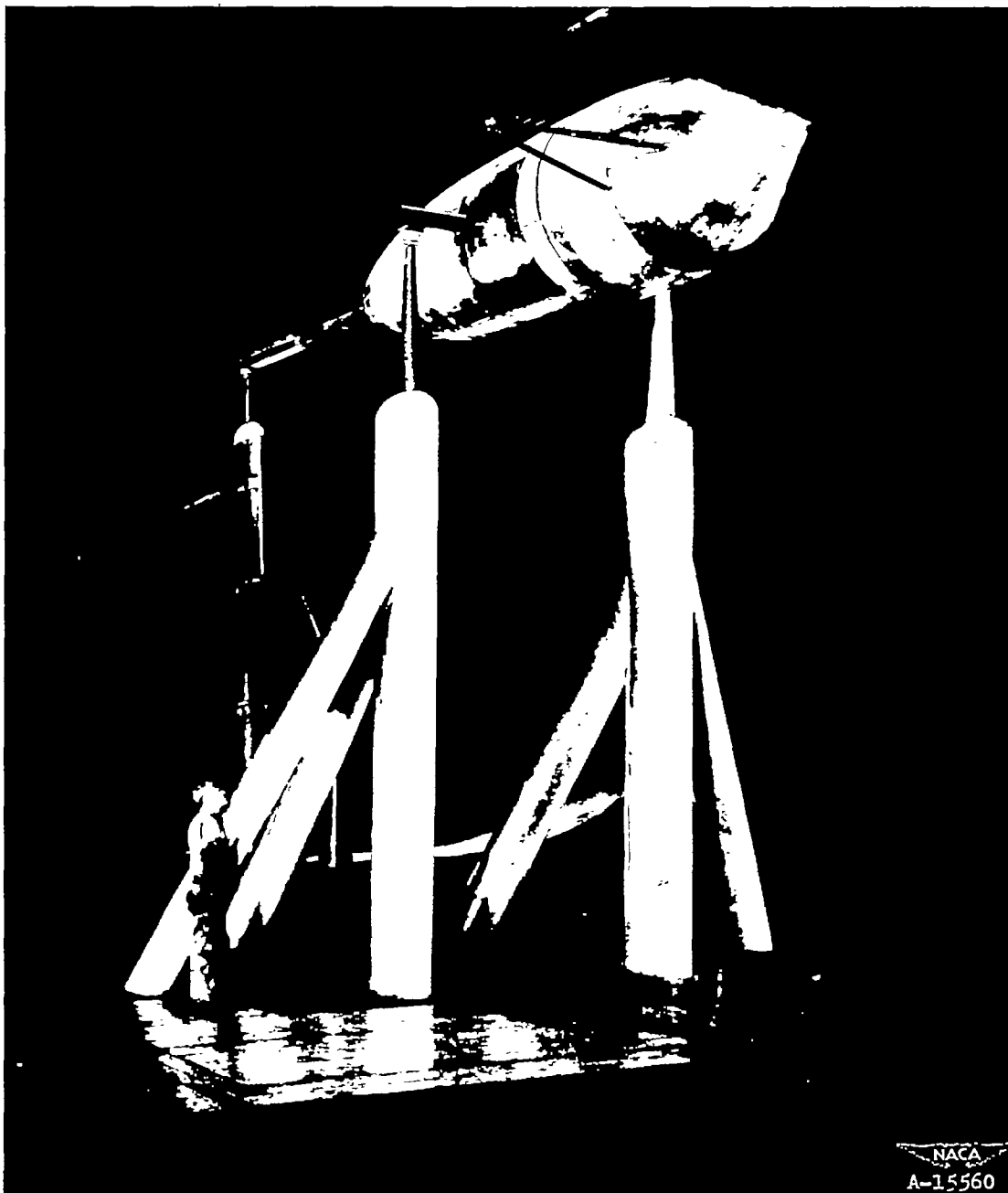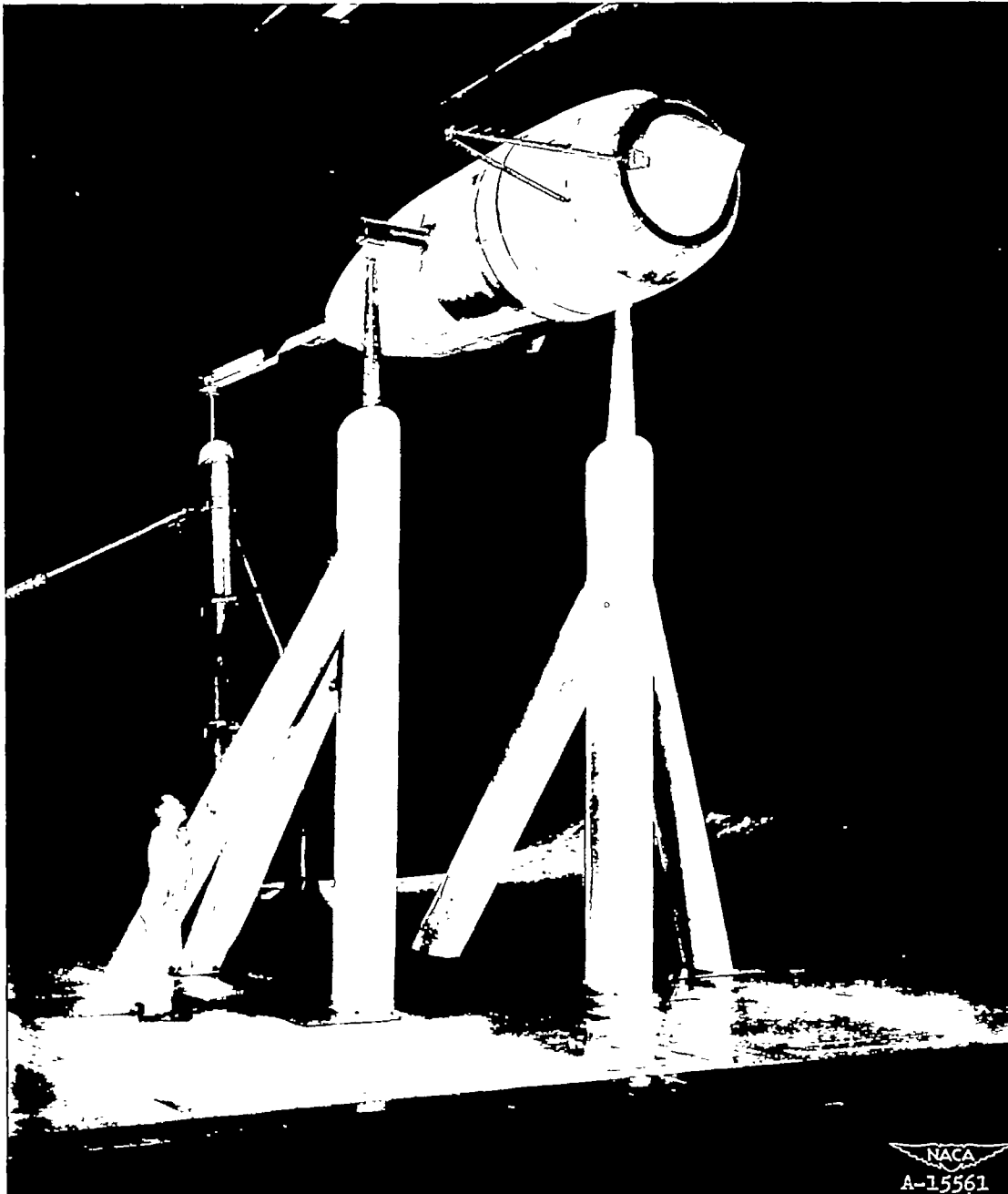(c) Nacelle with conical spinner.

Figure 3.- Concluded.

(a) Basic Nacelle.

Figure 4.— The nacelles mounted in the Ames 40— by 80—foot wind tunnel.

(b) Nacelle with conical fairing.

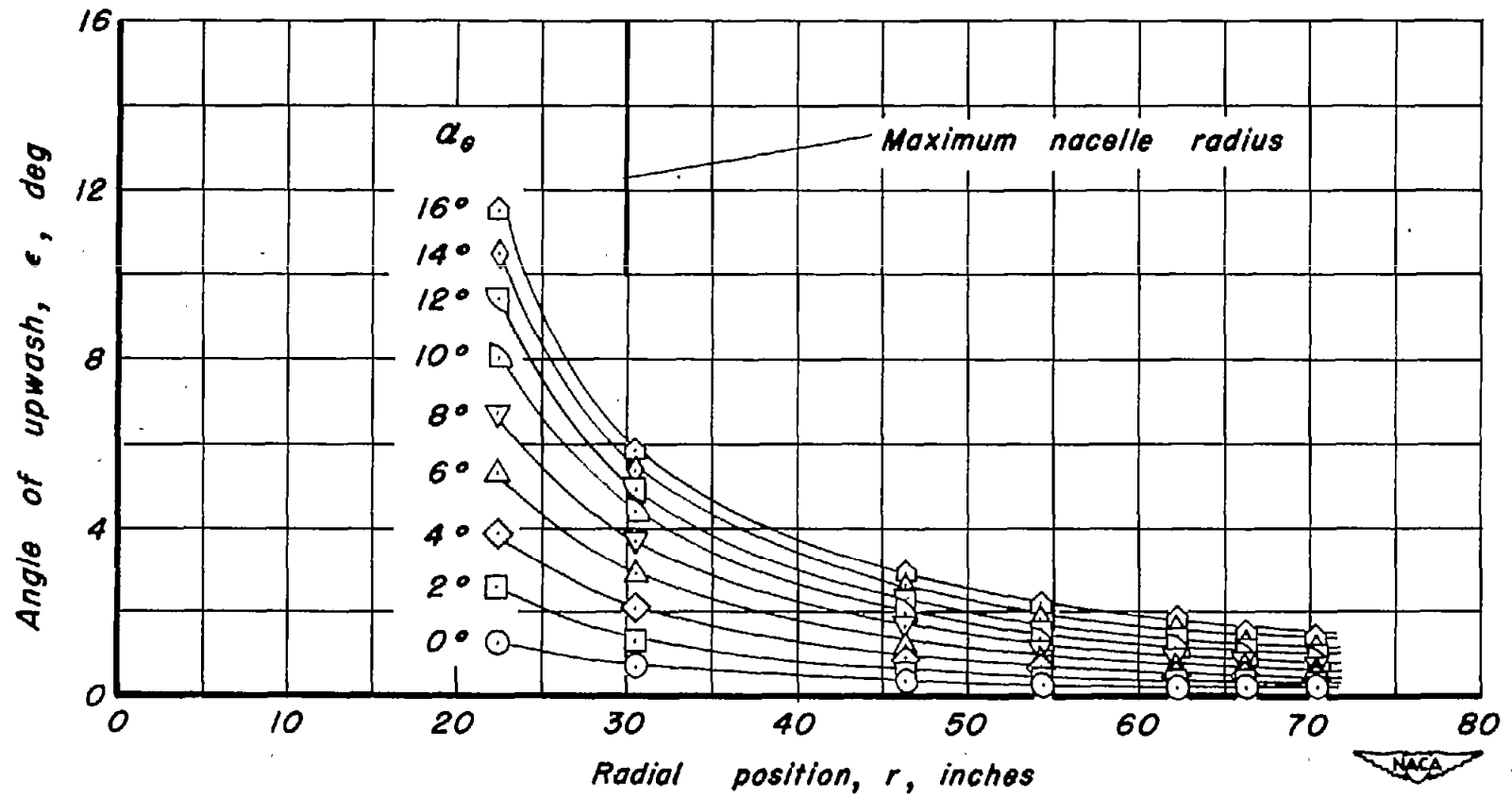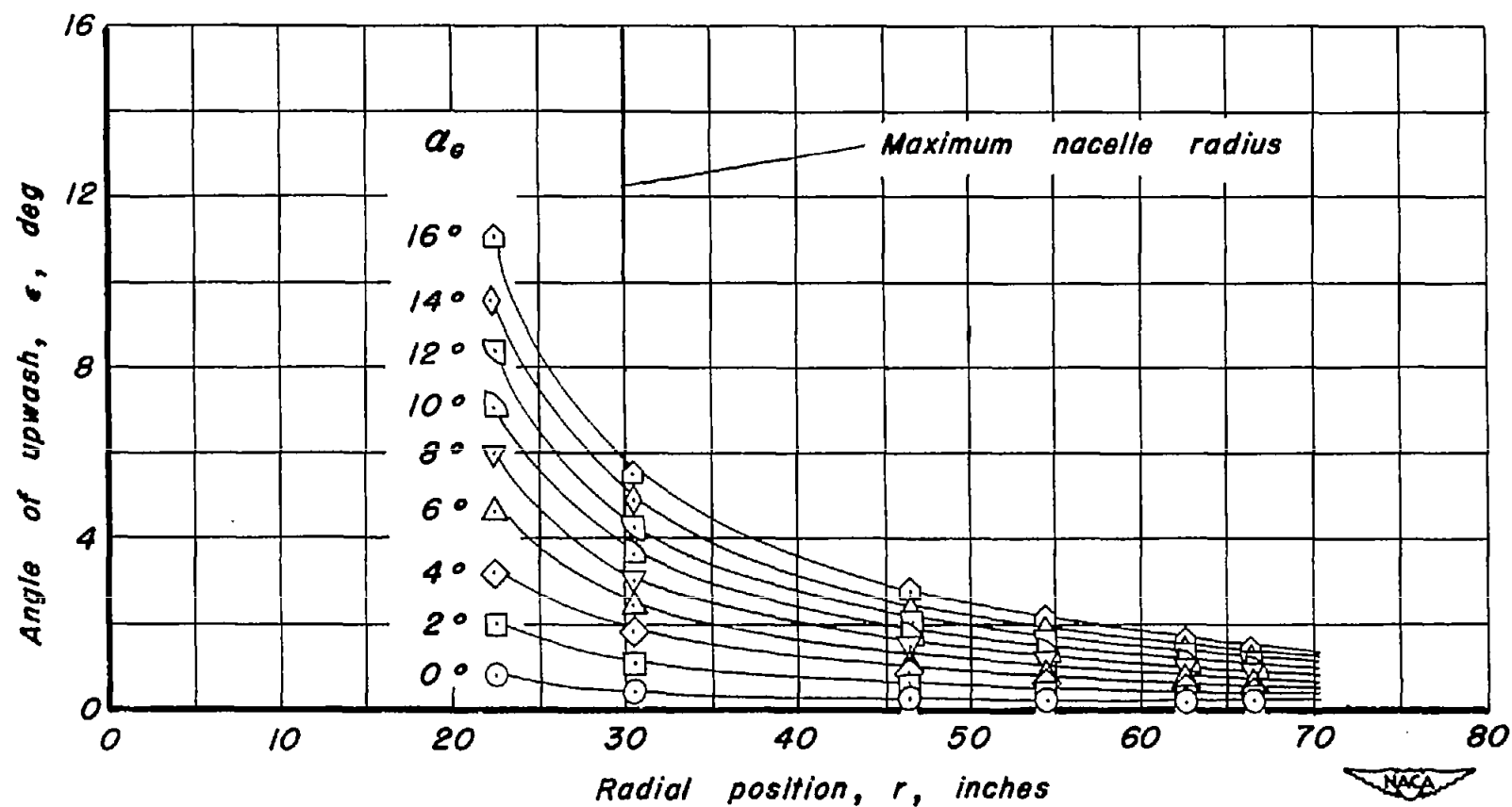Figure 4.— Continued.

(c) Nacelle with conical spinner.

Figure 4.— Concluded.

(a) Basic nacelle.
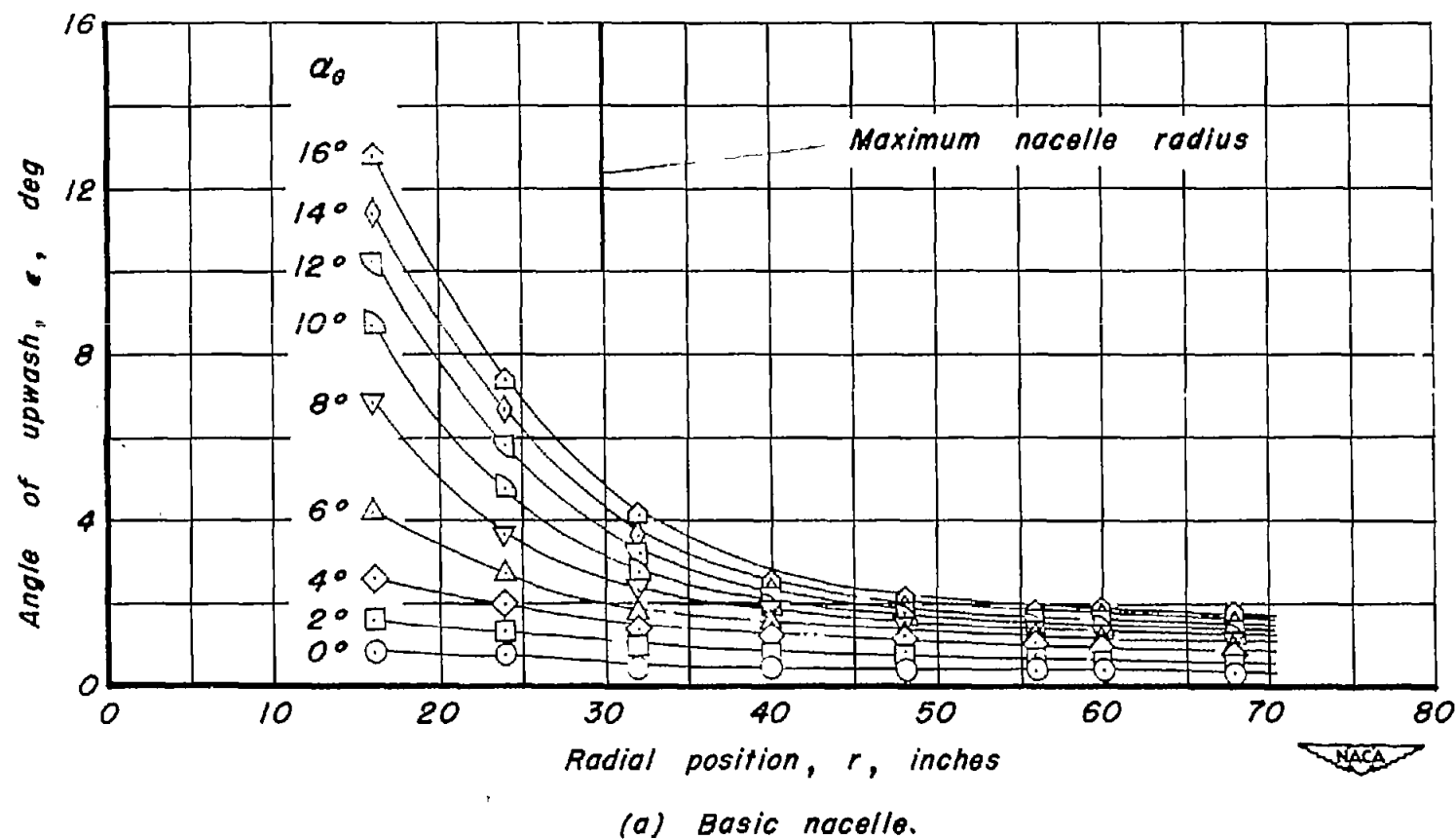
Figure 5. — Variation of the angle of upwash at the horizontal center line of the survey disk for several angles of attack.

(b)   Nacelle with conical fairing.

Figure 5. — Continued.

(c) Nacelle with conical spinner.
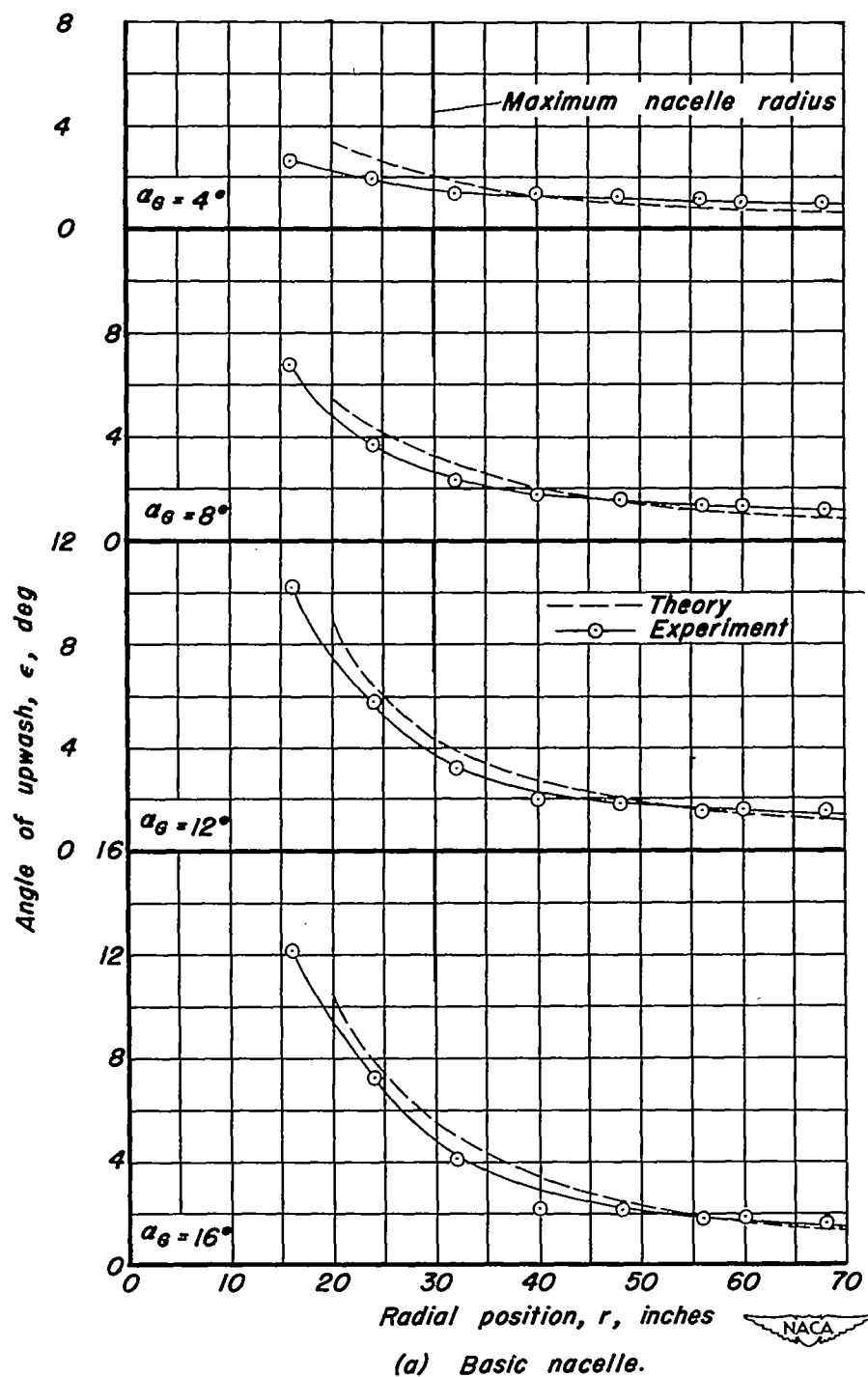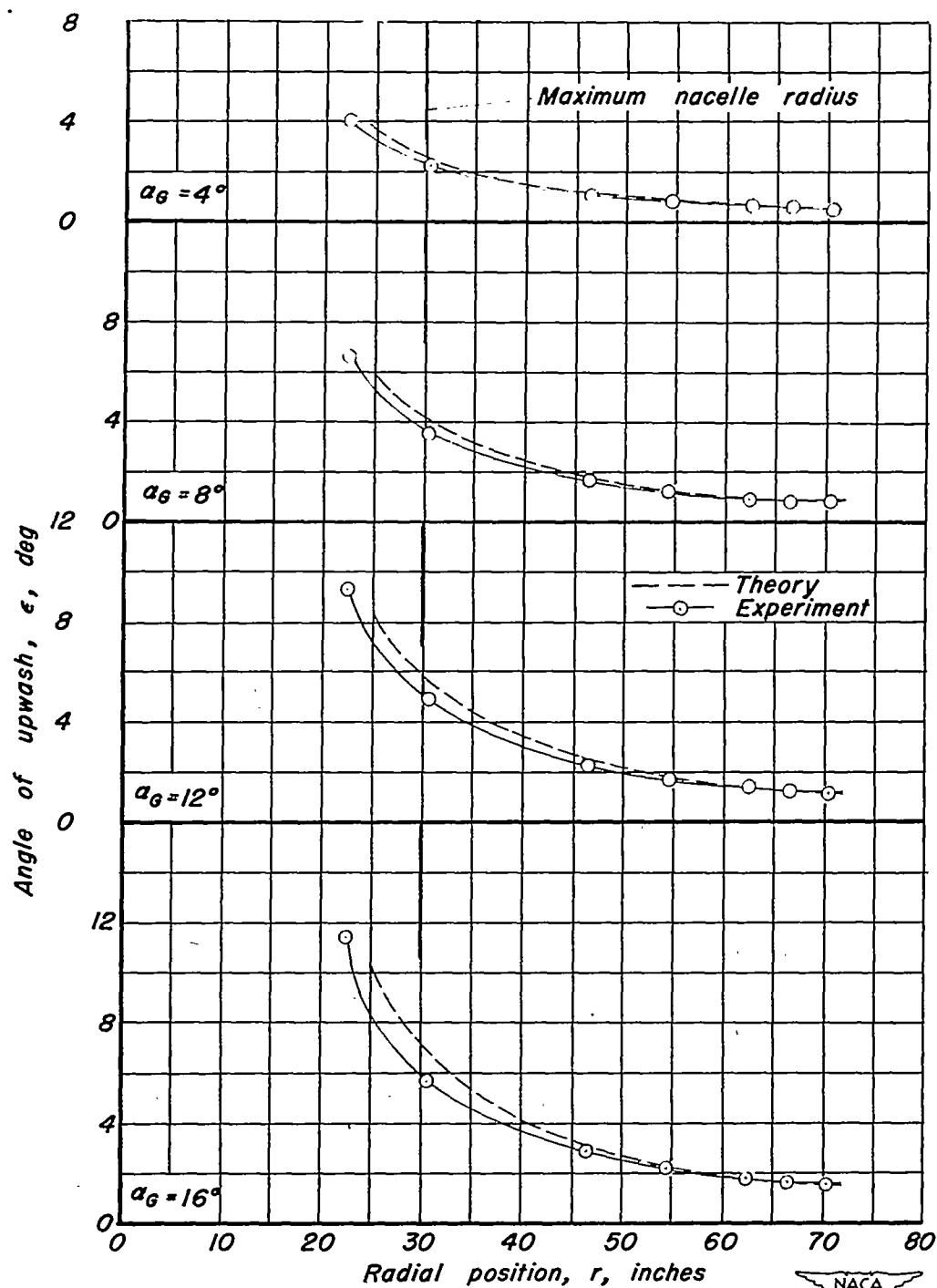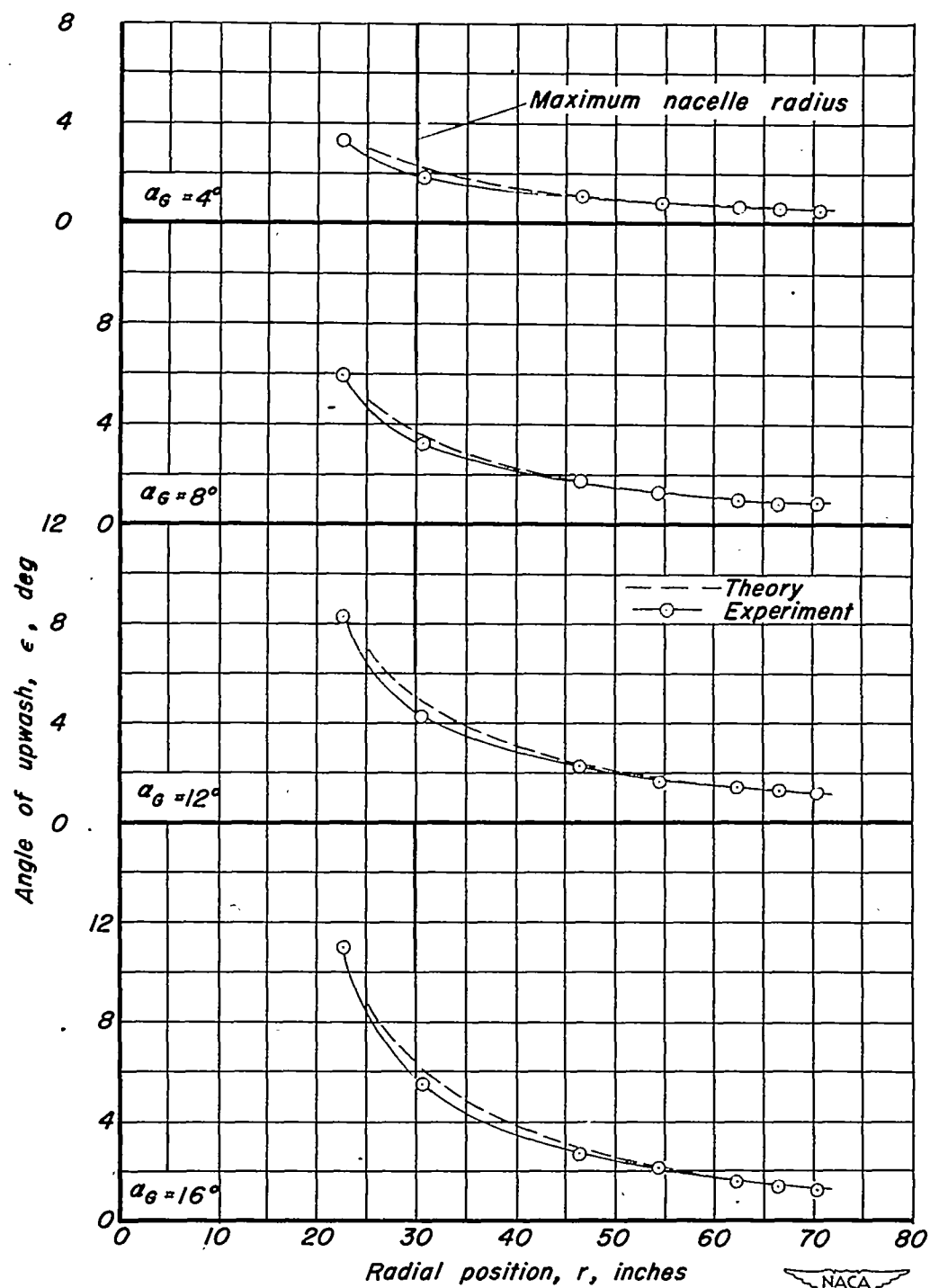
Figure 5. - Concluded.

(a) Basic nacelle.

Figure 6.— Comparison of measured and computed var-
iations of the angle of upwash at the horizontal
center line of the survey disk.

(b) Nacelle with conical fairing.

Figure 6.- Continued.

(c) Nacelle with conical spinner.
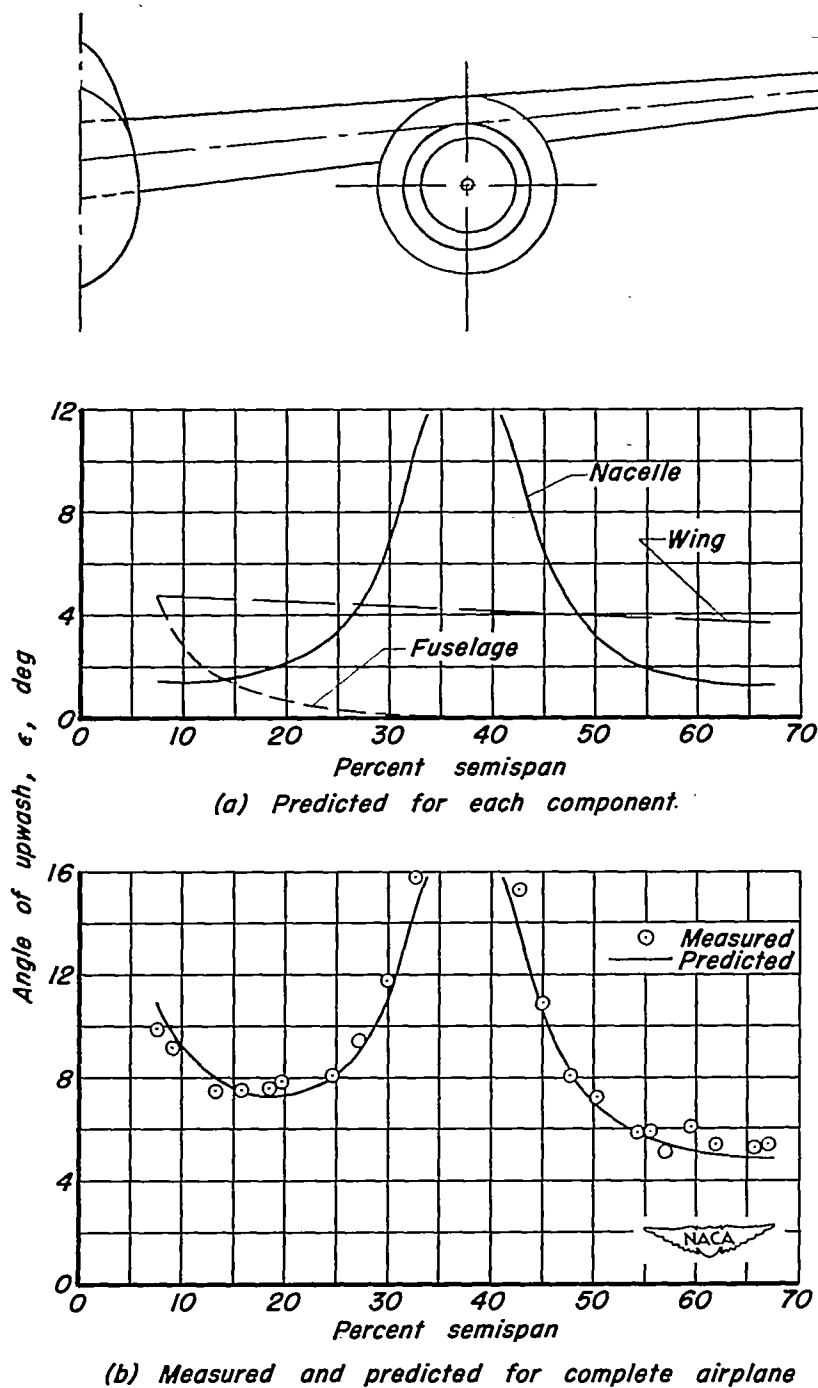
Figure 6. - Concluded.

(a) Predicted for each component.

(b) Measured and predicted for complete airplane

Figure 7.- Variation of the angle of upwash at the horizontal center line of the survey disk of the airplane of reference 1. $a_G = 10°$.